



## **Removal of Arsenic from Simulated Groundwater using Calcined Shale as the Adsorbent**

**N'Da Akoua Alice Koua-Koffi<sup>1\*</sup>, Lassina Sandotin Coulibaly<sup>1</sup>, Drissa Sangare<sup>1</sup> and Lacina Coulibaly<sup>1,2</sup>**

<sup>1</sup>*UFR - Ingénierie Agronomique, Forestière et Environnementale, Département de Environnement et Développement Durable, Université de Man, BPV 40 Man, Côte d'Ivoire.*

<sup>2</sup>*Unité de Biotechnologie et Ingénierie de l'Environnement, Unité de Formation et de Recherche en Sciences et Gestion de l'Environnement (UFR-SGE) Université Nangui Abrogoua, 02 BP 801 Abidjan 02, Abidjan, Côte d'Ivoire.*

### **Authors' contributions**

*This work was carried out in collaboration among all authors. All authors read and approved the final manuscript.*

### **Article Information**

DOI: 10.9734/IRJPAC/2021/v22i630414

*Editor(s):*

(1) Dr. Farzaneh Mohamadpour, University of Sistan and Baluchestan, Iran.

*Reviewers:*

(1) Manzoor Ahmed Sanjrani, Donghua University, Shanghai, China.

(2) Mahmoud A Rabah, Central Metallurgical research and development Institute, Egypt.

Complete Peer review History: <https://www.sdiarticle4.com/review-history/69166>

**Original Research Article**

**Received 17 May 2021**

**Accepted 23 July 2021**

**Published 04 August 2021**

### **ABSTRACT**

Well water intended for human consumption in the Akouédo area (Ivory Coast) contained arsenic at a concentration average above 0.01 mg/L, WHO guideline value. The shale was used as an adsorbent for the removal of arsenic from these waters. This shale was collected in Lomo Nord in Ivory Coast, washed then dried at a temperature of 60°C and finally calcined in an oven at several temperatures: 200°C, 300°C, 400°C, 500°C, 600°C and 700°C. X-ray diffraction, Fourier transform infrared spectroscopy (FTIR) and thermal analysis (TGA-DSC) were used to characterize the fraction of uncalcined and calcined shale powder. Batch mode tests were performed with water containing arsenic in order to study the influence of contact time, initial concentration and pH on the adsorption of arsenic on calcined shale. The results showed that shale calcined at 300°C could remove 99.41% of arsenic in water. The treated water meets the World Health Organization (WHO) standard for drinking water. Regarding the kinetic data, 0.034 mg/g of arsenic was adsorbed on the calcined shale within 7 hours. At pH 8, the maximum reduction rate was estimated up to 96%. The pseudo-second order model is the most appropriate of all the models applied to describe the kinetic data. This study shows that slate shale calcined at 300°C could be used as a low cost adsorbent to remove arsenic from Akouédo well water for consumption.

\*Corresponding author: E-mail: alyss\_akoua@yahoo.fr;

**Keywords:** Arsenic; calcined shale; adsorption; temperature.

## 1. INTRODUCTION

Arsenic (As) is the 20<sup>th</sup> most abundant element in the earth's crust and is found in all environmental matrices (soil, water, air and living matter) [1,2]. The arsenic contents in the water vary according to the lithology crossed, the climate and the anthropogenic contribution [3]. The consumption of water from aquifers contaminated with arsenic is a global public health problem [4,5]. Arsenic is classified by the World Health Organization (WHO) as a potent carcinogen. The WHO states that drinking water contain no more than 0.01 mg/L [6]. Arsenic concentrations higher than the WHO recommendations for drinking water were noted by Mangoua-Allali et al. [7], in the Akouédo area in Ivory Coast. The presence of arsenic in these waters could endanger the health of populations. In the literature, various arsenic depollution techniques have been studied [8,9,10]. However, most of these techniques are expensive for developing countries and require skilled labor, hence the need to search for locally available materials to remove arsenic from drinking water. In recent years, local materials like laterite, shale, clay, illite, kaolinite and pozzolan have been used to remove arsenic from the water [11,12,13,14]. Speaking of local materials, natural shale has been used as an adsorbent to remove arsenic from water by Koua-koffi et al. [15]. Its results gave reductions in arsenic in water but not always below the WHO guideline values depending on the concentrations treated. It appears important to optimize the potential of shale by thermal treatment to assess the effect of the treatment and its impact on the elimination of arsenic. The main objective of this study is to determine the optimum temperature for calcination of the shale and the mineralogy of the shale which could play a role in adsorption. Then assess the possibility of using calcined shale powder to remove arsenic from drinking water. Finally, use kinetic models to fit the data.

## 2. MATERIALS AND METHODS

### 2.1. Material

#### 2.1.1 Shale

In this research, shale used is local natural material collected at Lomo Nord, in Ivory Coast (Center). It was washed several times to remove earthy matter and finally rinsed with distilled water. Then, the samples were crushed and

sieved to have a desired particles size (less than 80 µm) using a Saulas NF.X 11.501 sieve. It has been calcined at different temperatures, such as 200°C, 300°C, 400°C, 500°C, 600°C and 700°C for 2h, and used to conduct the adsorption of arsenic in a batch at room temperature (25°C).

### 2.1.2 Adsorbate

As (III) stock solution (1000 mg/L) was prepared by dissolving reagent grade As (III) oxide of 99.5% purified into deionized water. The volume of the solution was made up to 1L in the bottle. The working solutions containing arsenic were prepared by dissolving appropriate amount of arsenic from stock solutions in well water. The pH of well water varied from 6.3 to 6.6 [15]. The experiments were performed at ambient temperatures up to 25°C.

## 2.2 Experimental Methods

### 2.2.1 Mineralogical analyses

Calcined and uncalcined shale have been characterised by Fourier Transform Infrared (FTIR) spectroscopy (Bruker Alpha-p) in the spectral range of 400 and 4000 cm<sup>-1</sup>, by X-ray diffraction (XRD) to identify the mineralogical phases, and by thermal analysis (TGA-DSC).

### 2.2.2 Adsorption experiments

Arsenic adsorption was undertaken in batch experiments. Solution prepared below was diluted to prepare the desired experimental concentrations. Arsenic sorption kinetics was evaluated at three initial concentrations (1; 5; 10 mg/L). Before each kinetic experiment, a given amount of adsorbent was put in bottles (500 mL) [15]. Then 40 ml of initial arsenic solution was added. The samples were agitated with rotary shaker (Retsch, Berlin) at 200 rpm for 24 h. The pH was maintained at 7 and, if necessary, adjusted by using 0.1 M NaOH or 0.1 M HCl solution. The effect of pH on arsenic adsorption was examined in a series of experiments using the initial arsenic concentration of 5 mg/L at pH 4, 5, 6, 7, 8, 9 or 10. The acidic or alkaline pH was controlled by adding the required amounts of dilute hydrochloric acid (HCl) or sodium hydroxide (NaOH) solutions. The pH of the sample was determined using a pH meter (Multiparameter pH meter Edge HI 2020-01). The solutions were stirred during 12 hours and then,

the concentration of arsenic in the solution was measured. After filtration through a 0.45 µm cellulosic acetate film, the arsenic concentration of the filtered solutions was analyzed with Optical Emission Spectrometer OPTIMA 2100 Dual View (ICP-OES 2100 DV). The arsenic adsorbed percentage was calculated using this relation (1).

$$\% \text{ As (III)adsorbed} = \frac{(C_0 - C_f)}{C_0} * 100 \quad (1)$$

The amount of arsenic adsorption at any time  $t$ ,  $q_t$  (mg/g), was calculated according to Equation (2):

$$q_t = \frac{(C_0 - C_f)}{m} * V \quad (2)$$

where:  $C_0$  (mg/L) = Initial arsenic concentrations,  $C_f$  (mg/L) = Equilibrium arsenic concentrations,  $V$  (L) = Volume of the as solutions,  $m$  (g) = Adsorbent mass,  $q_t$ (mg/g) = Adsorption capacity.

First-order, pseudo-second-order and Weber's intraparticle diffusion models are the kinetic models used here.

The first-order rate equation is as follows equation (3):  $\log (q_e - q_t) = \log q_e - \frac{K_1}{2.303} * t$

The pseudo-second-order model equation is given as equation (4) :  $\frac{t}{q_t} = \frac{1}{k_2 q_e^2} + \frac{t}{q_e}$

The Weber's intraparticle diffusion model [16] can be expressed by the following equation:  $q(t) = K_d t^{0.5} + C$

### 3. RESULTS AND DISCUSSION

#### 3.1 Characterization of Shale

The X-ray spectra of raw and heat-treated shale reveal six main minerals which are quartz, muscovite, chlorite, kaolinite, albite and dolomite (Fig. 1). First, well crystallized quartz with lines at 4.25; 3.34; 2.45; 2.28; 2.24; 2.13; 1.82 and 1.67 Å. Then comes the muscovite (line at 10.03, 4.99, 4.46, 3.89, 2.88, 2.8 Å). Chlorite is presented by its characteristic peak at 14.28 Å. The presence of kaolinite is marked by its peaks at 7.18 Å; 3.55 Å and 2.46 Å; 2.53 Å and 1.98 Å. Albite is present at its peak at 3.18 Å and dolomite is detected at 2.98 Å. The diffractogram of shale calcined at 400°C shows decreases in intensity at certain peaks of kaolinite (7.18 and 3.55 Å) and albite (3.18 Å). The identification of the minerals contained in the shale helps to

understand and justify the reduction of arsenic in water.

The characteristic spectra of raw and calcined shale (Fig. 2) crushed have absorption bands around 3696; 3652 cm<sup>-1</sup> due to proton elongation vibrations that represent kaolinite. Kaolinite-related OH deformation vibrations are also observed at 1019 and 913 cm<sup>-1</sup> [17]. OH elongation vibration at 3596 cm<sup>-1</sup> is attributed to chlorite. 778 band is identified as a band specific to quartz deformation vibrations. Finally, the Si-O deformation vibrations associated with albite can be identified in the 744 and 649 cm<sup>-1</sup> bands. The identified albite, kaolinite and dolomite are said to be potentially favorable minerals for arsenic retention. Decreasing these minerals could reduce arsenic adsorption. On the spectrum of shale calcined at 400°C, there is a reduction in intensity of bands attributable to kaolinite and albite. FTIR analysis confirmed the presence of minerals already observed by XRD. Similar results were reported by other authors while studying phosphate sorption on shale [11,17].

ATG-DSC of shale has 3 large areas of distinct mass loss and endothermic peaks (Fig. 3). A loss of mass of the order of 1.04% marked by endothermic peaks occurs around 56°C. The second weight loss is 0.12% at 216°C. Finally, the third mass loss is 0.84% with an endothermic peak observed around 484°C. After calcination, the losses of mass and voids formed by the departure of water and the thermal decomposition of organic components would lead to an increase in porosity and a greater specific surface area so as to promote significant adsorption of arsenic. The characterization by DRX, IR and ATG-DSC of the shale reveals the presence of important minerals which allow the reduction of the arsenic of the water.

#### 3.2 Arsenic Adsorption Characteristics (Effect of Calcination Temperature, Optimal Contact Time, Initial Concentration and pH Effects)

##### 3.2.1 Effect of calcination temperature on the adsorption of arsenic

Arsenic adsorption of using calcined shale at different temperatures ranging from 200°C up to 700°C (Fig. 4), showed a high percentage of arsenic removal. The arsenic removed from calcined shale decreases after 300°C, hence the percentage of adsorption which goes from 99.41% down to 64 % for initial arsenic concentration of 5 mg/L. The temperature of

300°C is the best calcination temperature. The efficiency of the material at this temperature would result from the various transformations produced during heating (appearance of defects in the structure of the material, voids due to the departure of water and the thermal

decomposition of organic components). Similar calcination temperature of material for arsenic removal was reported by Weidner and Ciesielczyk [18]. This temperature of 300°C which gave best adsorption results was used for the other investigations.

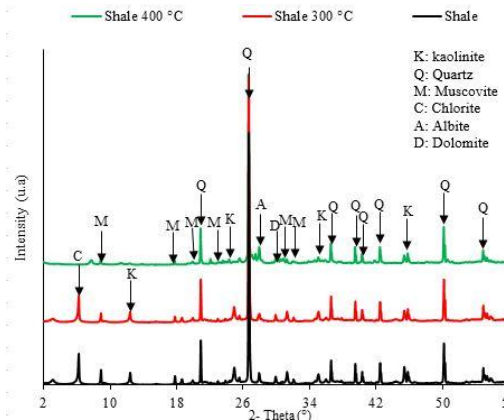


**Fig. 1. X-ray diffraction patterns of Lomo-Nord black Calcined and uncalcined shale**

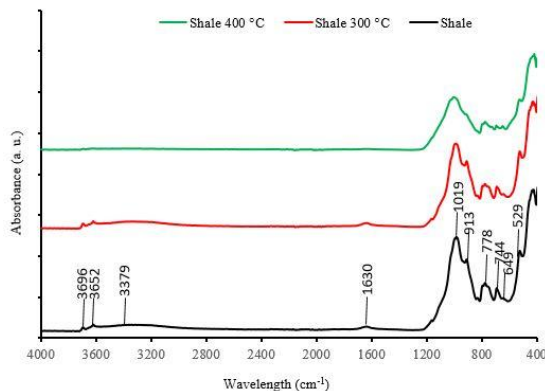


**Fig. 2. FTIR spectrum of Lomo-nord black calcined and uncalcined shale**

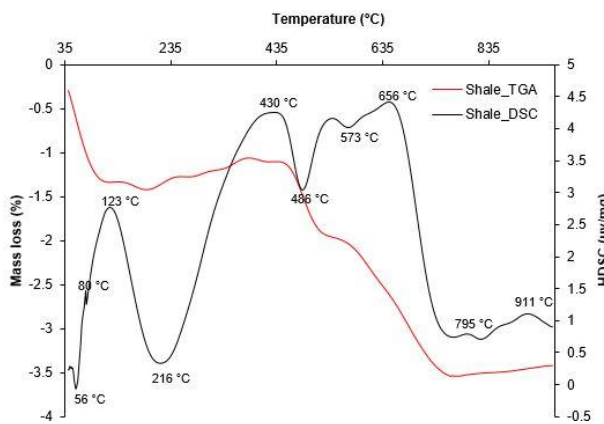


**Fig. 3. TGA- DSC spectrum of Lomo-nord black shale**

### 3.2.2 Optimal contact time and initial concentration effects and pH effects

The calcined shale curve has two (2) slopes (Fig. 5). The first few moments (0 to 15 min) of the reaction correspond to a very fast stage with a removal rate of 54%. Retention capacity ( $q$ ) goes from 0 to 0.018 mg/g of as after 15 minutes of stirring. Adsorption capacity values reach a maximum value after 7 h with a  $q_m = 0.034$  mg/g of As. The adsorption capacity with the calcined shale (0.034 mg/g) is greater than that obtained by Koua-Koffi et al. [15] with the same material used in a crude manner (0.02 mg/g). This difference would be due to the effect of the heat treatment which would have led to defects into the shale structure and the thermal decomposition of the organic matter which would increase the porosity. Equilibrium adsorption capacities increase and the percentage of elimination decreases with increasing as concentration and contact time. Orders of magnitude of adsorption capacity for shale calcined at 300°C are of 0.013; 0.034 and 0.08 mg/g as respectively for initial concentrations of 1; 5 and 10 mg/L. The increase in the adsorption capacity could be related to the increase of the concentration gradient. As for the percentage of elimination, its decrease with the increase of the concentration would be due to the progressive saturation of the material. Similar results have been reported by Udoeyo et al. [19]; Zhao et al. [20]; Chen et al. [21], who explained them by the same phenomenon.

### 3.2.3 pH effect

Fig. 6 illustrates the effect of the arsenic solution pH on the arsenic removal was studied in the pH range from 4 to 10. The elimination rate increases with the pH of 4 to 6. However, the retention capacity of as is maximum at pH 8 with a yield of 96%. The removal efficiency of shale calcined is found to decrease at higher pH from 8. The highly protonated surface of shale is not

favorable for As. The significant sorption of arsenic on calcined shale that contains clay minerals such as kaolinite, would be due to complexation phenomena [22,23].

### 3.3 Adsorption Kinetic

Kinetics models including the pseudo-first-order model of Lagergren, the pseudo-second-order model of Ritchie and the Weber's intraparticle diffusion model were tested for simulation of the experimental results (Fig. 7a, b). The best fit for the experimental data of this study was achieved by the application of a pseudo-second-order kinetic equation.

Adsorption kinetic parameters for the adsorption of arsenic by calcined shale are represented in table 1. The pseudo second-order model can be effectively used to predict the adsorption kinetic of arsenic by calcined shale. The good agreement with pseudo-second-order model demonstrated that the adsorption determining step may be the exchange of electrons between the adsorbent and the adsorbate or the valence forces through sharing [24,25]. The plot of the adsorption curves from the parameters obtained using the model shows the conformity between simulation and experimentation.

The plot of uptake, versus the square root of time of intraparticle diffusion model is presented by fig.7 c. The straight does not go through the origin and the values of the correlation coefficient are between 0.3 and 0.7. This indicates that intraparticulate diffusion is not the only limiting step, but other kinetic models can also control the adsorption rate. The plots corresponding to the initial arsenic concentration of 5 mg/L and 10 mg/l show two steps. The first step was ascribed to the diffusion of arsenic from the external solution to the external surface of calcined shale or instantaneous adsorption stage. The second step was the intraparticle diffusion [26].

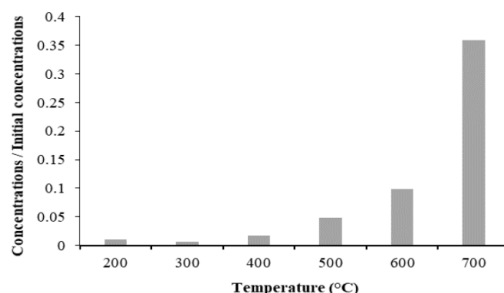


**Fig. 4. Effect of calcination temperature on the adsorption of arsenic**

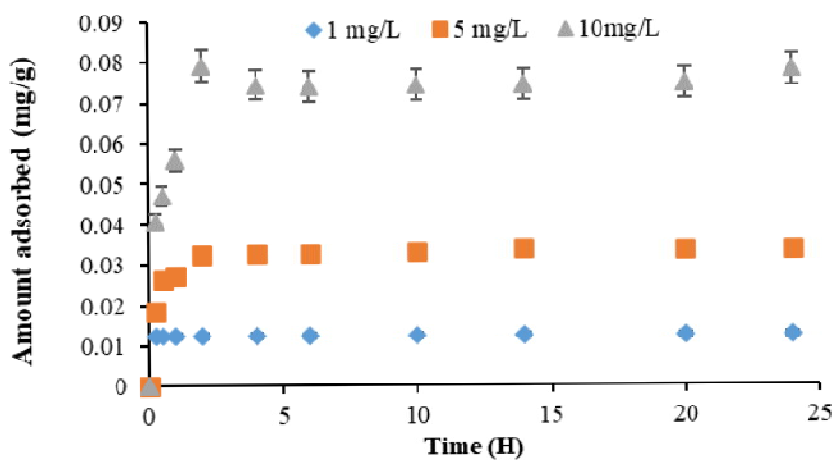


**Fig. 5. Arsenic adsorption on calcined shale: Effect of reaction time and initial arsenic concentration (Initial arsenic concentration 1, 5 and 10 mg/L, at 25°C, pH = 7 ± 0.5, agitation time: 24h)**

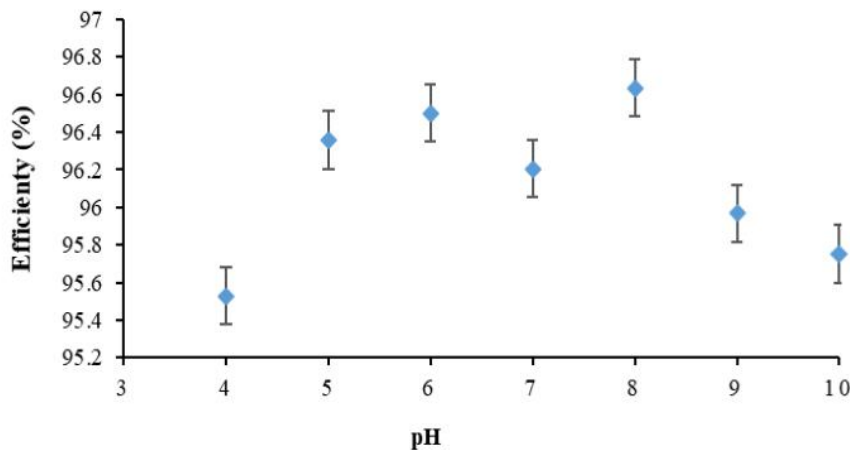


**Fig. 6. Arsenic removal as a function of pH. (Reactions conditions: Initial As concentration 5 mg/L, at 25°C, agitation time: 12h)**

**Table 1. Kinetic model parameters obtained from model fitting to experimental data**

Concentrations		1 mg/L	5 mg/L	10 mg/L
Pseudo-first-order kinetic model	$q_{e,exp}$ (mg As/g)	0.013	0.034	0.082
	$q_{e,cal}$ (mg As /g)	0.041	0.094	0.107
	$k_1$ ( $\text{h}^{-1}$ )	$9.10^{-4}$	0.121	0.043
	R	0.16	0.77	0.16
Pseudo-second-order kinetic model	$q_{e,cal}$ (mg As /g)	0.012	0.034	0.079
	$k_2$	9054.5	195.05	49.92
	R	1	0.99	0.99
Intra-particle diffusion model	$k_d$ ( $\text{mg}/\text{h}^{1/2} \text{ g}$ )	$7.10^{-6}$	0.002	0.006
	C	0.012	0.024	0.054
	R	0.32	0.73	0.72

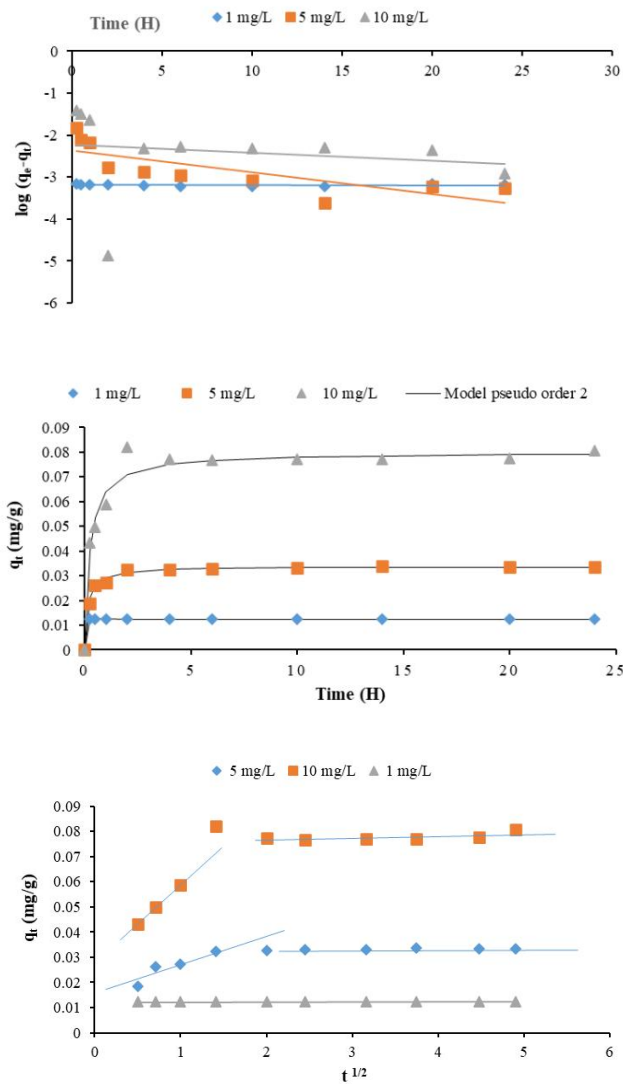


**Fig.7. Kinetic model analyses for the arsenic adsorption onto calcined shale in the solution of different initial concentrations (1 mg As/L, 5 mg As/L and 10 mg As/L) (a) pseudo-first-order model, (b) pseudo-second-order model (c) intra-particle diffusion model**

### 3. CONCLUSION

The calcined shale contained clay as its major component, it is an important element for the adsorption of arsenic. When shale calcined at 300°C, the highest arsenic removal of 99% was demonstrated. This arsenic removal rate is higher than that obtained when testing with the same gross material which gave 76%. Calcined shale was successful in removing arsenic from water. Treated water satisfied the WHO standard for drinking water. The arsenic adsorption capacity increased with both the increasing initial arsenic concentration and the contact time, but

equilibrium is reached after an agitation time of 7 hours. The kinetics of arsenic adsorption is best described by the pseudo-second-order kinetic model for calcined shale. These results suggest that calcined shale has the possibility to be adapted for small-scale application. Further investigation of arsenic adsorption in the column will confirm the applicability of calcined shale as an adsorbent in the removal of arsenic.

### COMPETING INTERESTS

Authors have declared that no competing interests exist.

## REFERENCES

1. Nisticòa R, Celi LR, Prevot AB, Carlos L, Magnacca G, Zanzo E, Martin M. Sustainable magnet-responsive nanomaterials for the removal of arsenic from contaminated water. *J Hazard Mater.* 2018;342:260-269.
2. Sommella A, Deacon C, Norton G, Pigna M, Violante A, Meharg AA. Total arsenic, inorganic arsenic, and other elements concentrations in Italian rice grain varies with origin and type. *Environ Pollut.* 2013;181:38-43.
3. Ahoulé DG, Lalanne F, Mendret J, Brosillon S, Maïga AH. Arsenic in african waters: A review. *Water Air Soil Pollut.* 2015;226(9):1-13.
4. Nzihou JF, Bouda M, Hamidou S, Diarra J. Arsenic in drinking water toxicological risk assessment in the North region of Burkina Faso. *J. Water Res. Prot.* 2013;5:46-52.
5. Wang C, Luo H, Zhang Z, Wu Y, Zhang J, Chen S. Removal of As(III) and As(V) from aqueous solutions using nanoscale zero valent iron-reduced graphite oxide modified composites. *J. Hazard. Mater.* 2014;268:124-131.
6. OMS Guidelines for drinking-water quality: 4th ed. incorporating the first addendum. OMS, Geneva, Switzerland. 2017;564.
7. Mangoua-Allali ALC, Koua-Koffi A, Akpo KS and Coulibaly L. Evaluation of Water and Sanitation Situation of Rural Area near Landfill, Abidjan. *Journal of Chemical, Biological and physical sciences.* 2015;5 (3):3033-3041.
8. Sarkar A, Paul B. The global menace of arsenic and its conventional remediation—a critical review. *Chemosphere.* 2016; 158:37-49.
9. Andrade LH, Aguiar AO, Pires WL, Miranda G, ATexeira LPT, Almeida GCC, Amaral MCS. Nanofiltration and reverse osmosis applied to gold mining effluent treatment and reuse. *Braz J Chem Eng.* 2017;34(1):93-107.
10. Fazi S, Amalfitano S, Casentini B, Davolos D, Pietrangeli B, Crognale S, Rossetti SArsenic removal from naturally contaminated waters: a review of methods combining chemical and biological treatments. *Rendiconti Lincei.* 2015;27(1):51-58.
11. Mar KK, Karnawati D, Sarto, Putra DPE, Igarashi T, Tabelin CB. Comparison of Arsenic Adsorption on Lignite, Bentonite, Shale, and Iron Sand from Indonesia. *Procedia Earth and Planetary Science.* 2013;6:242-250.
12. Kofa GP, Ndikoungou S, Kayem GJ, KAMGA R. Adsorption of arsenic by natural pozzolan in a fixed bed: Determination of operating conditions and modelling. *J Water Process Eng.* 2015; 6:166-173.
13. Maiti A, Basu JK, De S. Experimental and kinetic modeling of as (V) and as (III) adsorption on treated laterite using synthetic and contaminated groundwater: Effects of phosphate, silicate and carbonate ions. *Chem Eng J.* 2012;191: 1-12.
14. Omera OS, Husseina BHM, Mohammed AH, Arbi M. Mixture of illite-kaolinite for efficient water purification: removal of As (III) from aqueous solutions. *Desalin Water Treat.* 2017;79: 273-281.
15. Koua-Koffi N, Coulibaly L, Sangare D, and Coulibaly L. Laterite, Sandstone and Shale as Adsorbents for the Removal of Arsenic from Water. *Am J Analyt Chem.* 2018; 9(7):340-352.  
DOI:10.4236/ajac.2018.97027.
16. Weber WJ, and Morris JC. Kinetics of adsorption on carbon from solution. *J Sanit Eng Div Am Soc Civ Eng.* 1963; 89:31-60.
17. Coulibaly SL, Yvon J, and Coulibaly L. Physicochemical Characterization of Lomo Nord black shale and application as low cost material for phosphate adsorption in aqueous solution. *J Environ Earth Sci.* 2015;5:42-60.
18. Weidner E, Ciesielczyk F. Review Removal of Hazardous Oxyanions from the Environment Using Metal-Oxide-Based Materials. *Materials.* 2019;12:927.
19. Udoeyo FF, Brooks R, Inyang H, Bae S. Imo lateritic soil as a sorbent for heavy metals. *IJRAS.* 2010;4(1):1-6.
20. Zhao F-J, McGrath SP. and Meharg AA. Arsenic as a food chain contaminant: mechanisms of plant uptake and metabolism and mitigation strategies. *Annu Rev Plant Biol.* 2010;61:535-559.
21. Chen N, Zhang ZY, Feng CP, Li M, Chen RZ, and Sugiura N. Investigations on the batch and fixed-bed column performance of fluoride adsorption by Kanuma mud. *Desalination.* 2011;268:76-82.
22. Glocheux Y, Pasarín MM, Albadarin AB, Allen SJ. & Walker GM. Removal of

- arsenic from groundwater by adsorption onto an acidified laterite by-product. Chem Eng J. 2013;228:565-574.
23. Goldberg S. Competitive adsorption of arsenate and arsenite on oxides and clay minerals. Soil Sci Soc Am J. 2002;66: 413-421.
24. Nemade PD, Kadam AM and Shankar HS. Adsorption of arsenic from aqueous solution on naturally available red soil. J Environ Biol. 2009;30(4):499-504.
25. Bhowmick S, Chakraborty S, Mondal P, Van-Renterghem W, Vanden-Berghe S, Roman-Ross G, Chatterjee D. & Iglesias M. Montmorillonite-supported nanoscale zero-valent iron for removal of arsenic from aqueous solution: Kinetics and mechanism. Chem Eng J. 2014;243: 14-23.
26. Dawood S and Sen TK. Removal of anionic dye congo red from aqueous solution by raw pine and acid-treated pine cone powder as adsorbent: equilibrium, thermodynamic, kinetics, mechanism and process design. Water Res. 2012;46: 1933-1946.

© 2021 Koua-Koffi et al.; This is an Open Access article distributed under the terms of the Creative Commons Attribution License (<http://creativecommons.org/licenses/by/4.0>), which permits unrestricted use, distribution, and reproduction in any medium, provided the original work is properly cited.

*Peer-review history:*

The peer review history for this paper can be accessed here:  
<https://www.sdiarticle4.com/review-history/69166>